Supplementary Information

Continuous Gas-to-Liquid Conversion for Carbon-Efficient Electroreduction of CO_2

Chengao Zhou, Hao Shen*, Zimin He, Canhui Wang, Buwei Hou, Yulin Liu, Xiaoyu Wang, Jinyi Zhang, Fei Xu, Fan Bu, Chao Wang*

Ralph O'Connor Sustainable Energy Institute and Department of Chemical and Biomolecular Engineering, Johns Hopkins University, Baltimore, MD, USA

* Correspondence: chaowang@jhu.edu; haoshen@jhu.edu

Experimental Methods

Chemicals. Argon (Ar. ≥99.9%), Carbon Dioxide (CO_2. ≥99.999%), and Hydrogen (H_2. ≥99.99%) were supplied by Airgas. Sodium Bicarbonate ($NaHCO_3$, ≥99.7%), Sodium Carbonate (Na_2CO_3, ≥99.5%), Bismuth (Bi, 45-μm powder, ≥99.5%), Tin oxide (SnO_2, 100-nm powder, ≥99%), 2-propanol ($(CH_3)_2CHOH$, anhydrous, ≥99.5%) were purchased from Sigma-Aldrich. Proton exchange ionomer dispersion (Nafion, D2020CS) and gas diffusion electrode (SIGRACET, 39BB) were purchased from Ion Power Inc. Anion exchange membrane (FuMA-Tech, FAB-PK-130) and anion exchange ionomer dispersion (FuMA-Tech, FAA-3-SOLUT-10) were purchased from Fuel Cell Store. Anion exchange ionomer dispersion (Sustainion, XA-9) was purchased from Dioxide Materials. Ultrapure water was used for all experiments and generated in the lab by a water purification system (Milli-Q, IQ 7000). All chemicals were used without additional purification and the ion-exchange membranes were activated following manufacturers' instruction before use.

Preparation of Catalyst-Loaded Electrode for CO_2 Electroreduction. Working electrodes for the electroreduction of CO_2 were prepared by drop-casting Bi and SnO_2 powder (dispersed in 2-propanol by sonication, pre-mixed with ionomer dispersion at 1.0 μg-ionomer/g-catalyst) onto the gas diffusion electrode to a loading of 1.0 mg-catalyst/cm^2-electrode.

Material Characterization. Scanning electron microscopy (SEM) images were taken by aJSM-IT700HR Field Emission SEM. Transmission electron microscopy (TEM) images were acquired on FEI Talos 200SC FEG TEM. High-resolution transmission electron microscopy (HRTEM) images and corresponding EDX elemental maps were acquired with HD2700C STEM (Hitachi) equipped with a probe aberration corrector and Enfina spectrometer (Gatan). The TEM

measurements of the catalysts before and after electrochemical test were performed on the powders from scratching off the catalyst-loaded GDEs. X-ray diffraction analysis was performed on a Bruker D8 Focus diffractometer (40 kV, 40 mA, sealed Cu X-ray tube with Kα1 = 1.540596 Å and Kα2 = 1.544493 Å) with a Ni filter and a LynxEye position-sensitive detector at room temperature. The XRD measurements of the catalysts before and after electrochemical test were performed directly on the catalyst-loaded GDEs.

Electrocatalytic Studies. The electrocatalytic studies for ECO_2R performance were carried out with a custom-made gas-tight flow cell. An IrRuOx-coated titanium screen was used as counter electrode and a saturated calomel (Hg/Hg_2Cl_2) electrode was used as reference electrode. Cathodic and anodic electrolytes were prepared by dissolving desired amount of $NaHCO_3$ (or Na_2CO_3) into ultrapure water. All electrolyte solution were bubbled with CO_2 (or Ar) to remove the O_2 before using in electrochemical test and kept in gas-tight bottle throughout the test. Both galvanostatic and potentiostatic experiments were performed with an Autolab 302 potentiostat (Metrohm). The gaseous reactants and products (CO_2, O_2, CO, H_2, etc.) were measured online using a gas chromatograph-mass spectrometry (GC-MS) instrument (Shimadzu) and the soluble products were collected and analyzed by a nuclear magnetic resonance (NMR) spectrometer (Bruker). All potentials discussed in this work were converted to the RHE scale via

$$E\ (vs.RHE)\ =\ E\ (vs.Hg/Hg_2Cl_2)\ +\ 0.27\,V\ +\ 0.0592\,V\ \times\ pH$$

The Faradic Efficiency (FE) of specific liquid product was calculated by following the equation:

$$FE = \frac{Z * n * F}{Q}$$

where Z is the number of electrons exchanged, n is the number of moles of specific product calculated based on H-NMR data, F is Faradic constant (96485.33 C/mol), and Q is the passed charge (C).

The Faradic Efficiency (FE) of specific gas product was calculated by following the equation:

$$FE = \frac{Z * c * F}{Q * \mathrm{q}}$$

where Z is the number of electrons exchanged, c is the molar concentration of specific product calculated based on GC-MS data, F is Faradic constant (96485.33 C/mol), Q is the passed charge (C) and q is the gas flow rate measured at the inlet of GC using a mass flow meter.

System and Process Design. To achieve high CCEs, a system was designed and built to recirculate both the gas feeding and liquid electrolytes for the CO2 electrolyzer with controlled pressure and mass flow rates. The system was comprised of a gas flow looping subsystem and a liquid flow looping subsystem. For the gas looping subsystem, the electrolyzer outlet was connected to a cold trap (BVV), a compressor (Welch) and a buffering cylinder (Restek) before recirculated back to the electrolyzer. Control devices including mass flow controllers (MFC), mass flow meters (MFM) and pressure controllers (PC) from Alicat were installed in the looping system to maintain a constant pressure and mass flow rate. For the liquid looping subsystem, all electrolysis outlets were directly recirculated using a multi-channel peristaltic pump (Cole-Parmer). For anolyte, 0.1 mol/L of Na_2CO_3 was added to increase the buffering strength for the anodic reaction and offset the potential gradient-driven migration of carbonate anions across the membrane.[1] During the long-time operations, an aliquot of 250 mL was collected at every ~10 h for product analysis, which was replenished using fresh electrolyte.

Supplemental Figures

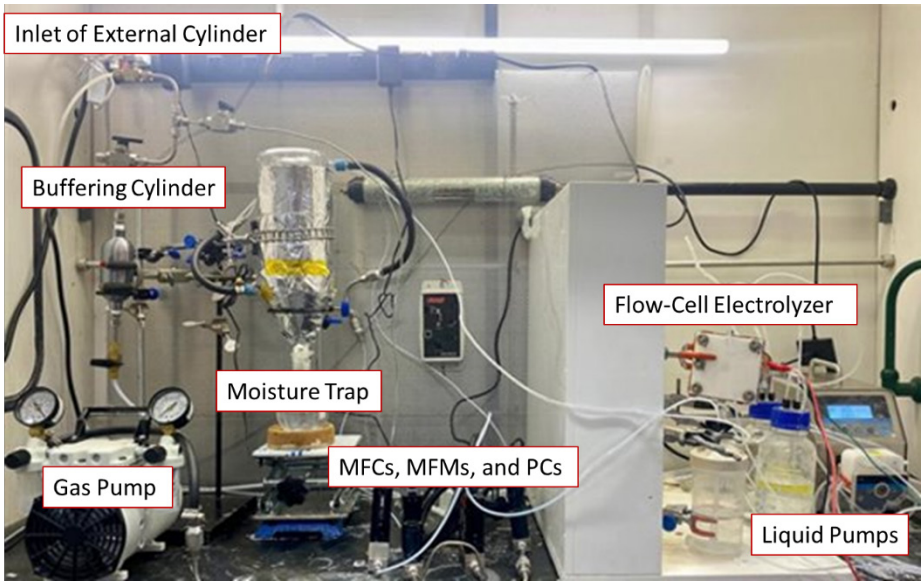

Figure S1. Photo of gas- and liquid-recirculated CO_2 reduction system.

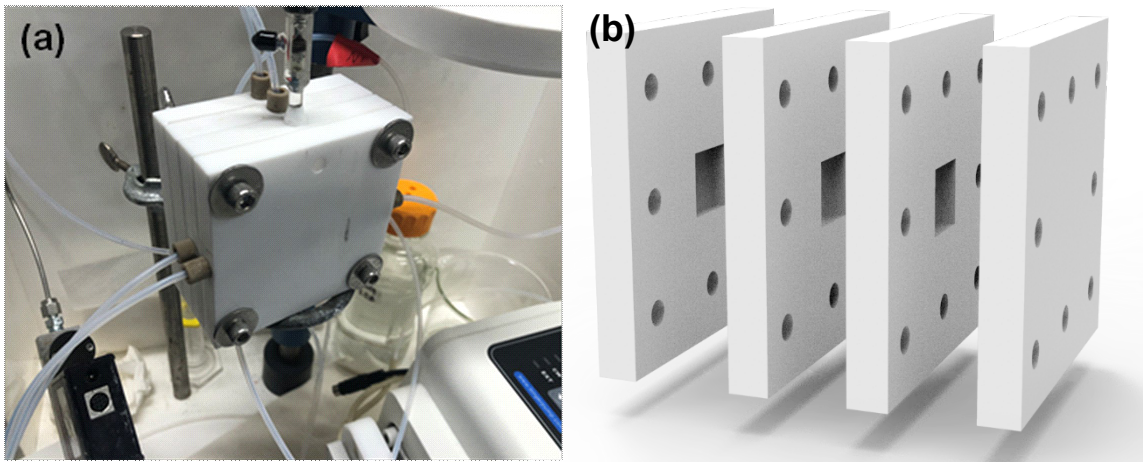

Figure S2. (a) Photo and (b) schematic drawing of the GDE-based flow cell used in this study.

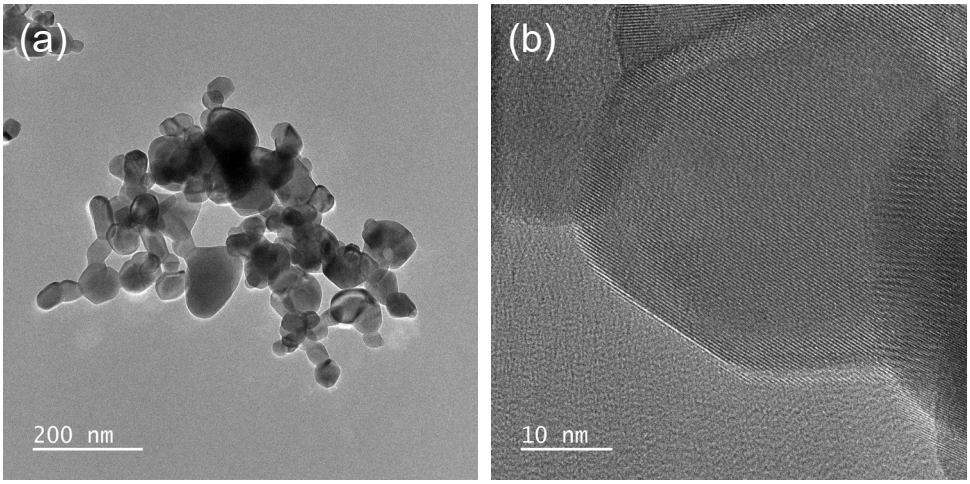

Figure S3. TEM Images of SnO_2 nanopowders.

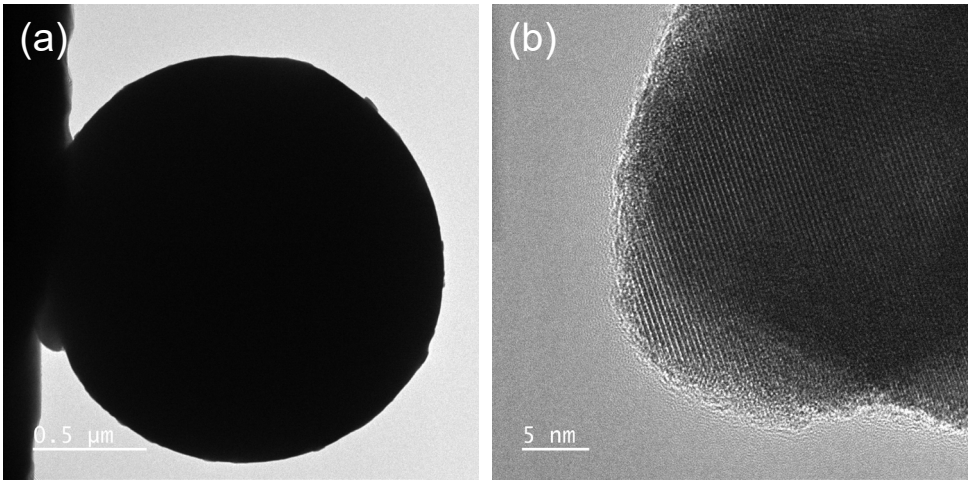

Figure S4. TEM Images of bismuth nanopowders.

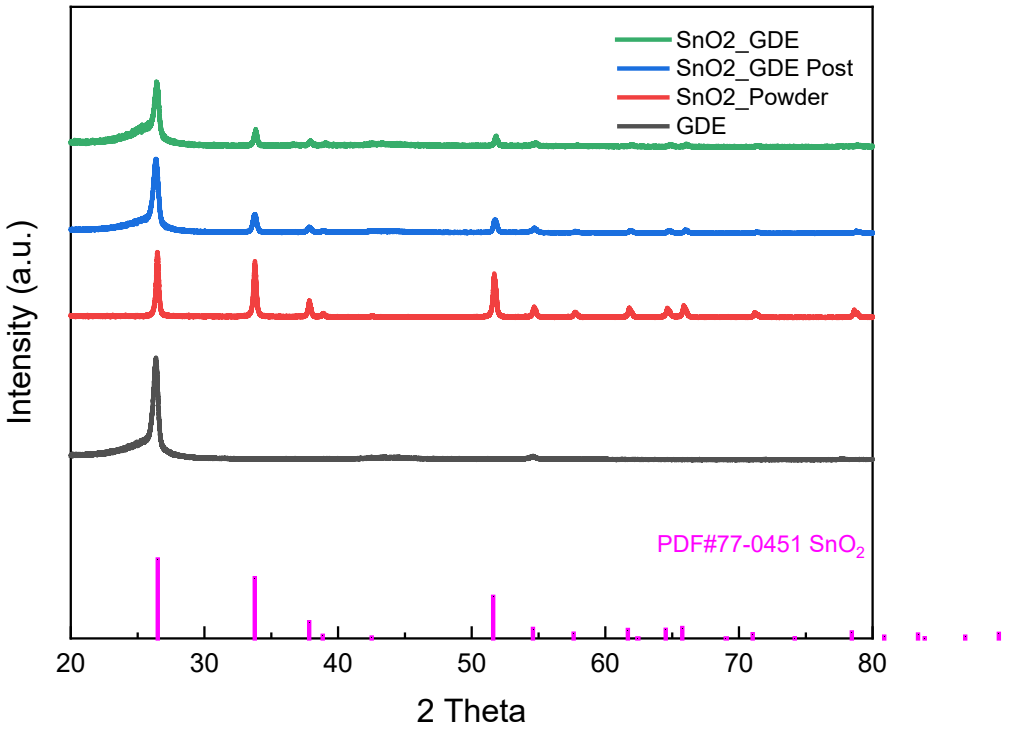

Figure S5. XRD of SnO_2 nanopowders and SnO_2-coated GDE electrode.

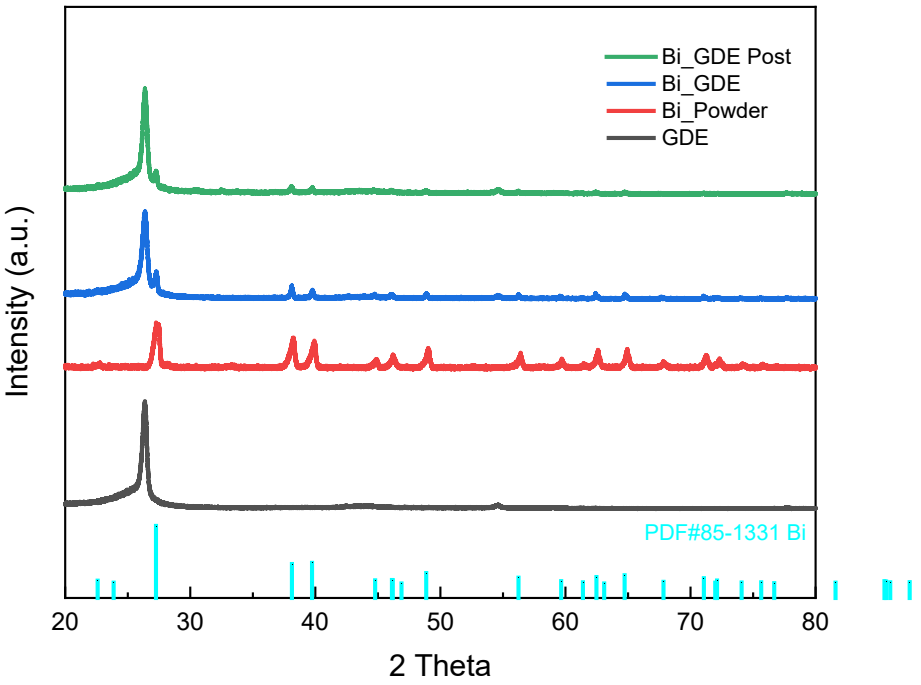

Figure S6. XRD of bismuth nanopowders and Bi-coated GDE electrode.

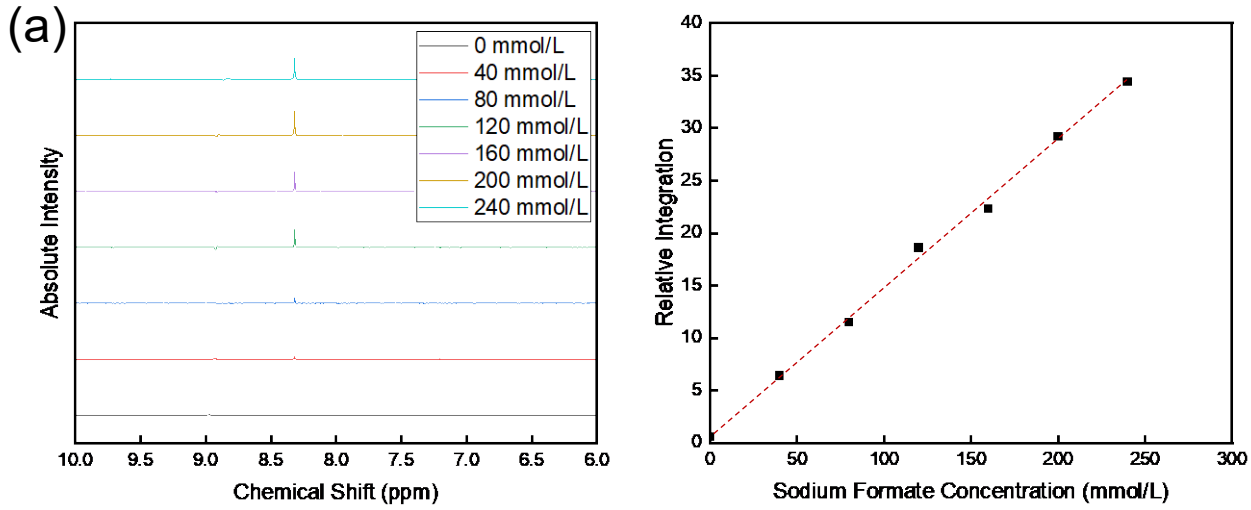

Figure S7. (a) H-NMR spectra for quantitative analysis of sodium formate concentration; (b) Calibration curve for quantitative analysis of sodium formate concentration.

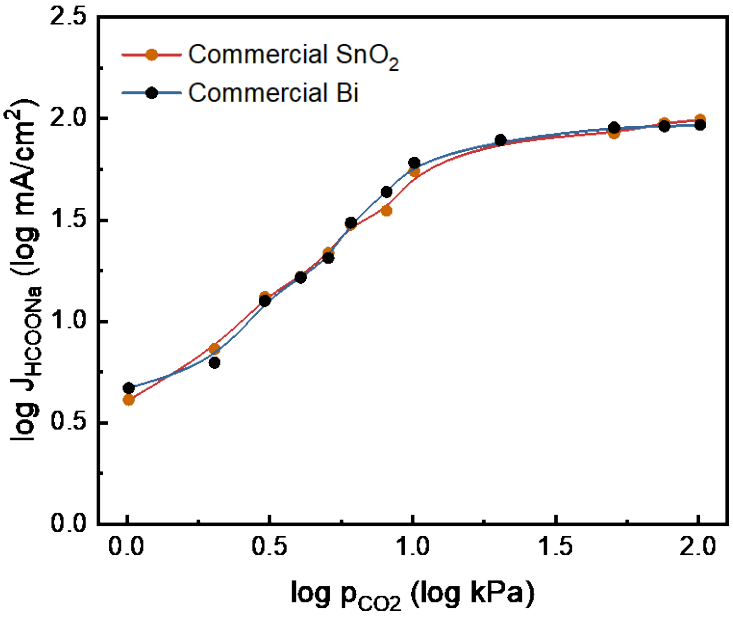

Figure S8. Reaction orders determined at −1.0 V for the electroreduction of CO_2 on commercial SnO_2 and commercial Bi.

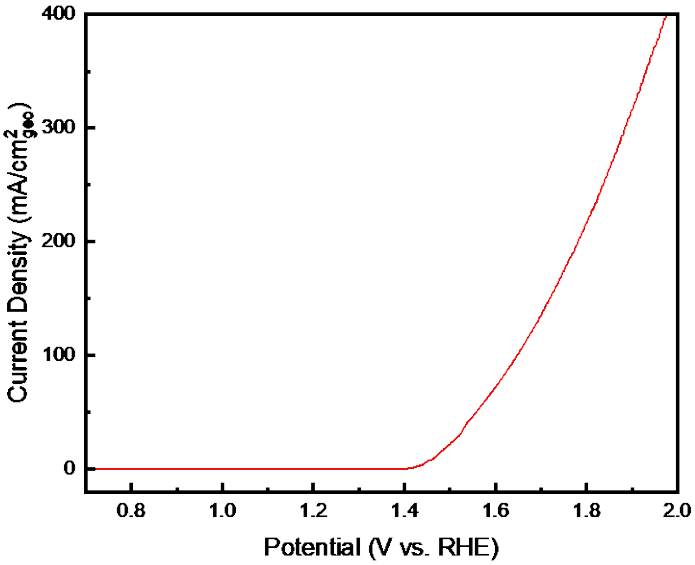

Figure S9. CV curve of DSA-based anode for OER reaction (scan rate: 10 mV/s, electrolyte: 1 mol/L $NaHCO_3$)

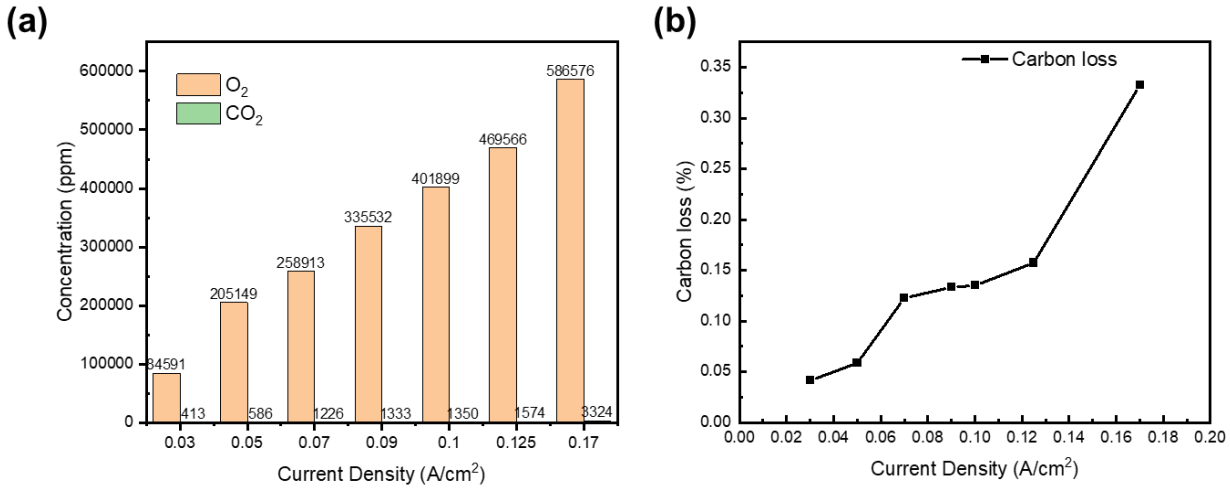

Figure S10. (a) O_2 and CO_2 concentration detected from the anode. (b) Ratio of anodic carbon loss in reference to the CO_2 feeding.

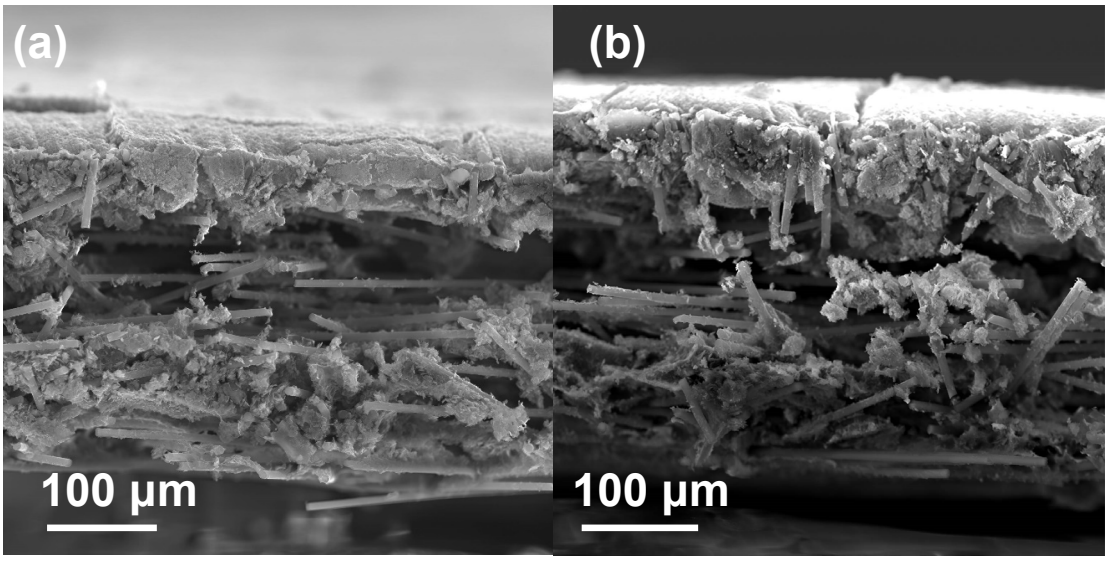

Figure S11. SEM photos of the cross section are of the post reaction GDE (a) Bi and (b) SnO_2

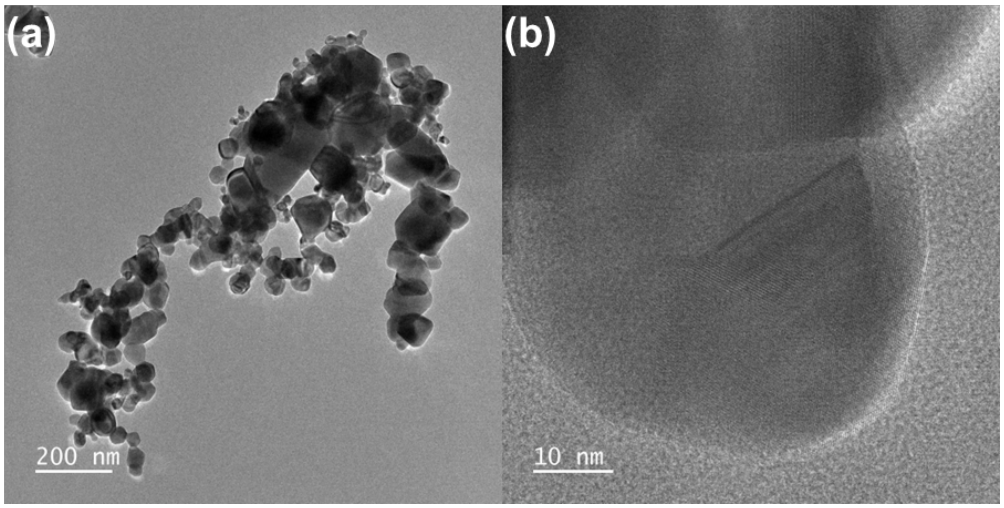

Figure S12. TEM photos of post reaction catalysts scraped from GDE after 66 hours test commercial SnO_2.

Figure S13. PSA, recirculation and CO_2 section in OPEX of the four configurations of CO2-to-fromate conversion plants.

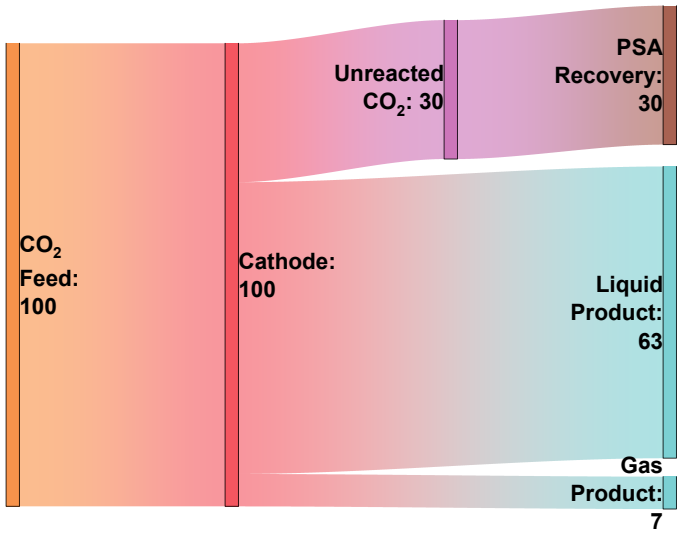

Figure S13. Mass flow in the BPM version.

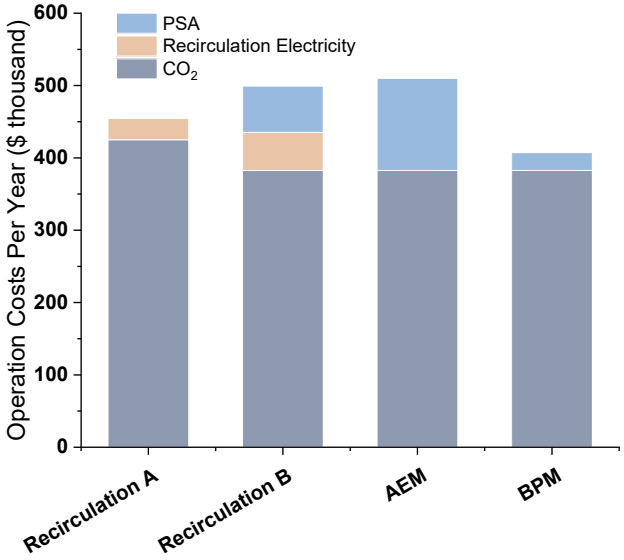

Figure S14. PSA, recirculation and CO_2 section in OPEX of four cases.

Mass Balance Analysis

Two cases are analyzed for the projected plant operations based on our circulating electrochemical system. *Recirculation A* considers the use of mixed $NaHCO_3$/Na_2CO_3 electrolyte with the following electrode reactions (similar to our experimental conditions, **Figure S15**)

Cathode: $CO_2 + NaHCO_3 + 2e^- \rightarrow HCOONa + CO_3^{2-}$

Anode: $2Na_2CO_3 + 2CO_3^{2-} + 2H_2O \rightarrow 4NaHCO_3 + O_2 + 4e^-$

Full Cell: $2CO_2 + 2H_2O + 2Na_2CO_3 \rightarrow 2HCOONa + 2NaHCO_3 + O_2$

where the $NaHCO_3$ in catholyte is converted into HCOONa and the Na_2CO_3 in anolyte is converted into $NaHCO_3$. It's assumed that the anodic oxygen evolution reaction is fully buffered at relatively low current densities. Formic acid is recovered from the catholyte via distillation[2-4]

$HCOONa + H_2O \rightarrow HCOOH + NaOH$

The produced NaOH is used to regenerate Na_2CO_3 via reaction with $NaHCO_3$

$NaOH + NaHCO_3 \rightarrow Na_2CO_3 + H_2O$

So, the overall reaction can be written as

$2CO_2 + 2H_2O \rightarrow 2HCOOH + O_2$

In principle, *Recirculation A* has 100% CCE, as there is no anodic carbon loss and the byproduct CO is recycled during "regeneration". In practice, some carbon loss due to gas leakage and anodic CO_2 evolution is inevitable for operation of the circulating system. This is in line with the high CCEs (>90% CCE) observed in our experimental studies (**Figure 4d**). The high CCEs of *Recirculation A* thus allows for the operation without gas separation for CO_2 recovery.

Alternatively, *Recirculation B* is considered for the operation with Na_2CO_3 as the electrolyte (**Figure S16**). It has been reported that bicarbonate or alkaline electrolytes turn into carbonate in steady-state operations of AEM-based CO_2 electrolyzers.[11] The CO_2-to-formate

conversion is somewhat different from the previously reported cases for charge-neutral products such as CO and ethylene, as the catholyte is always subjected to pH drop due to the formation of HCOONa. In this case, the electrochemical reactions can be written as

Cathode: $3CO_2 + H_2O + Na_2CO_3 + 4e^- \rightarrow 2HCOONa + 2CO_3^{2-}$

Anode: $2CO_3^{2-} \rightarrow 2CO_2 + O_2 + 4e^-$

Full Cell: $3CO_2 + H_2O + Na_2CO_3 \rightarrow 2HCOONa + 2CO_2 + O_2$

Here anodic carbon loss takes place when the oxygen evolution reaction goes beyond the buffering capacity of (bi)carbonate, which can be the case for operations at large current densities or after elongated operations without electrolyte replenishment.[12] Similar to *Recirculation A*, formic acid is recovered via distillation of the catholyte

$HCOONa + H_2O \rightarrow HCOOH + NaOH$

NaOH is also used to regenerate Na_2CO_3 but now via reaction with CO_2

$2NaOH + CO_2 \rightarrow Na_2CO_3 + H_2O$

So, the overall reaction can be written as

$4CO_2 + 2H_2O \rightarrow 2HCOOH + 2CO_2 + O_2$

It indicates that up to 50% of the CO_2 feeding is lost on the anode of the electrolyzer, resulting in a gas mixture of CO_2/O_2 with a molar ratio of 2/1. Thereby gas separation for CO_2 recovery is needed for the operation of *Recirculation B*.

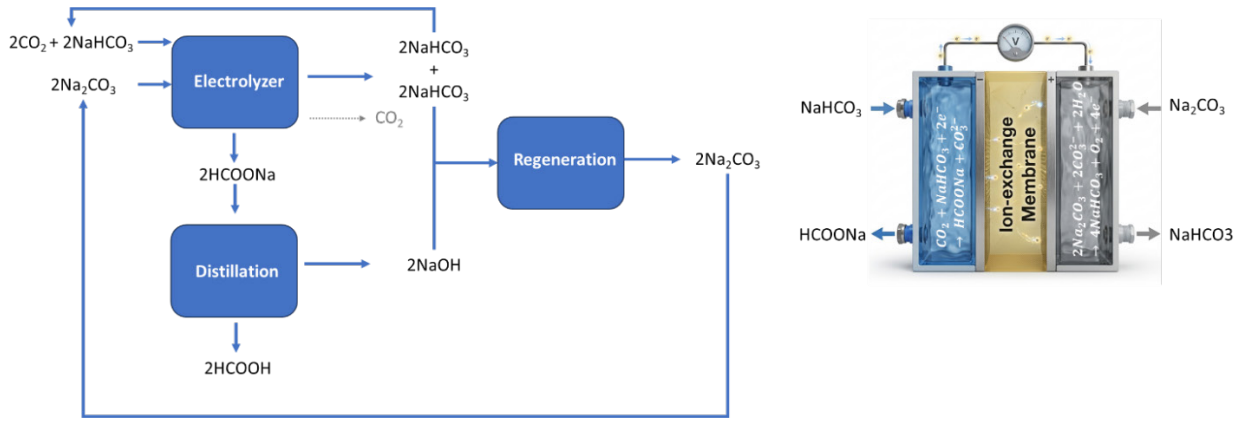

Figure S15. Process diagram showing the mass flow of *Recirculation A*.

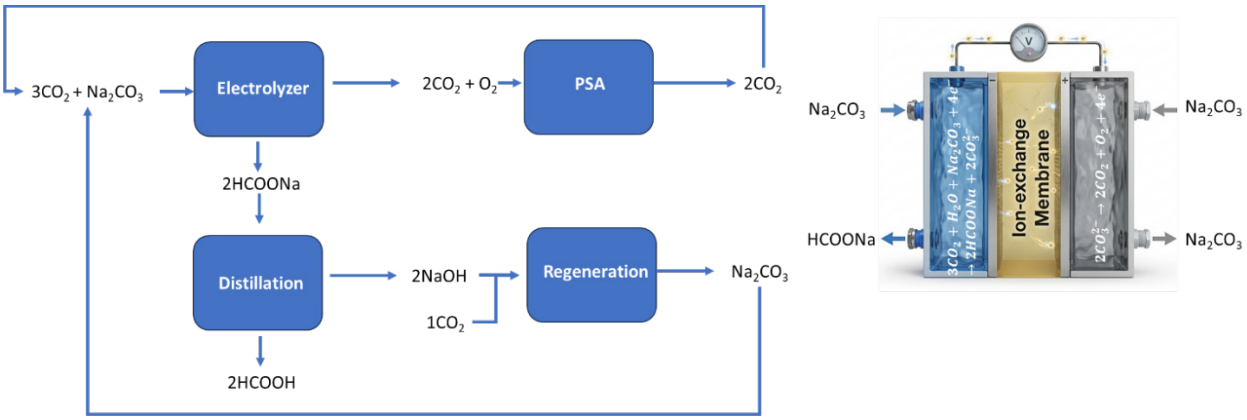

Figure S16. Process diagram showing the mass flow of *Recirculation B*.

Techno-Economic Analysis

All Capital Expenditures (CAPEX) were annualized using a capital recover factor (CRF) calculated from a discount rate of 10% and plant lifetime of 20 years. The levelized cost was calculated according to

$$Levelized\ Cost = \frac{AnnualizedCAPEX + AnnualOPEX}{AnnualFormateProduction}$$

$$Annualized\ CAPEX\ =\ Total\ CAPEX\ *\ CRF$$

The Operating Expenditures (OPEX) include electricity consumption of electrolyzer, electricity consumption of recirculation system, CO_2 feedstock, water, replacement of membranes & electrodes, electrolyzer maintenance, distillation of liquid product and pressure swing adsorption (PSA) for gas to recover CO_2.

The normalized cost of \$4,300 /m^2 is calculated based on the stack cost from the DOE Current Central H2A model (460 USD kW^{-1} at 1.75 V and 0.4 A cm^{-2}) and an installation factor of 1.12. Details can be found in the previous reports.[13,14] The cost of distillation, PSA and pump used for recirculation is calculated based on the reference unit with a scaling factor of 0.7[2,15]

$$\mathrm{C} = C_{\mathrm{ref}}\left(\frac{S}{S_{ref}}\right)^{n}$$

where

C= scaled equipment cost

C_{ref}= reference equipment cost

S= desired capacity (e.g., flow rate, throughput)

S_{ref}= reference capacity

n= scaling exponent

For this study:

$$n = 0.7$$

which reflects typical economy-of-scale behavior for chemical processing equipment.

Operation of *Recirculation A* follows the mass balance and process flow shown in **Figure S15**. This case saves the cost for PSA in CAPEX but pays 10% extra CO_2 for carbon loss in OPEX. Take the scale of 10,000 tonnes of formic acid production per year as an example (with a capacity factor of 350 days per year; same for *Recirculation B* below). The plant feeds 10,628.02 tonnes of CO_2 to the electrochemical cell, which generates 14,782.61 tonnes of HCOONa from CO_2 reduction. The electrochemical conversion is accompanied by consumption of 18,260.87 tonnes of $NaHCO_3$ in the catholyte and conversion of 23,043.48 tonnes of Na_2CO_3 into 36,521.74 tonnes of $NaHCO_3$ in the anolyte. Distillation of catholyte produces 10,000 tonnes of formic acid (corresponding to an overall CCE of 90%) and 8,695.653 tonnes of NaOH. From the 36,521.74 tonnes of $NaHCO_3$ derived from the analyte, half is circulated back to the electrochemical cell as catholyte, while the other half is used to react with NaOH to form 23,043.48 tonnes of Na_2CO_3. The latter is used to replenish anolyte for the electrolyzer.

In *Recirculation B*, PSA is included to recover CO_2 from the anodic gas products. Following the mass balance and process flow shown in **Figure S16**, the electrolyzer takes 14,347.8 tonnes of CO_2 and 11,521.7 tonnes of Na_2CO_3 as input to produce 14,782.6 tonnes of HCOONa and emits 9,565.2 tonnes of CO_2 from the anode. Distillation of the catholyte produces 10,000 tonnes of formic acid and 8 695.7 tonnes of NaOH. This NaOH stream is used to react with 4,782.6 tonne of CO_2 (considered as additional feedstock to the plant) and regenerate the 11,521.74 tonnes of Na_2CO_3 consumed in the electrolyzer. The 95,65.2 tonnes of CO_2 emitted from the anode is recovered via PSA and recycled back to the electrolyzer. Overall, the plant generates 10,000 tonnes of formic acid with net consumption of 95,65.2 tonnes of CO_2. It should be pointed here that the

electrochemical cell only has a CCE of 50% in *Recirculation B*, but with PSA for CO_2 recovery, the carbon utilization reaches 100% for the whole plant.

Table S1. Baseline parameters used in the TEA of the four types of CO_2 electrolyzer.

Parameter	Unit	Recirculation A	Recirculation B	AEM	BPM
Cell Voltage	V	2.5	2.5	2.5	3.3
Current Density	mA/cm^2	100	200	200	200
Formate FE	%	90%	85%	85%	85%
Electrochemical CCE	%	90%	50%	30%	70%

Supplemental References

1 Weng, L.-C., Bell, A. T. & Weber, A. Z. Towards membrane-electrode assembly systems for CO2 reduction: a modeling study. *Energy & Environmental Science* **12**, 1950-1968, doi:10.1039/c9ee00909d (2019).

2 Jouny, M., Luc, W. & Jiao, F. General Techno-Economic Analysis of CO2 Electrolysis Systems. *Industrial & Engineering Chemistry Research* **57**, 2165-2177, doi:10.1021/acs.iecr.7b03514 (2018).

3 Pérez-Fortes, M., Schöneberger, J. C., Boulamanti, A., Harrison, G. & Tzimas, E. Formic acid synthesis using CO2 as raw material: Techno-economic and environmental evaluation and market potential. *International Journal of Hydrogen Energy* **41**, 16444-16462, doi:10.1016/j.ijhydene.2016.05.199 (2016).

4 Gao, T. *et al.* Techno-economic Analysis and Carbon Footprint Accounting for Industrial CO2 Electrolysis Systems. *Energy & Fuels* **37**, 17997-18008, doi:10.1021/acs.energyfuels.3c01581 (2023).

5 Gutierrez, M. F., Lorenz, H. & Schulze, P. Carbon-Negative Production of Soda Ash: Process Development and Feasibility Evaluation. *Ind Eng Chem Res* **64**, 11474-11496, doi:10.1021/acs.iecr.5c00483 (2025).

6 Goh, W. *et al.* Techno-Economic Analysis of Mineralization and Utilization of CO2 in Recycled Concrete Aggregates. *Processes* **13**, doi:10.3390/pr13020410 (2025).

7 Lee, J. H., Lee, D. W., Kwak, C., Kang, K. & Lee, J. H. Technoeconomic and Environmental Evaluation of Sodium Bicarbonate Production Using CO2 from Flue Gas of a Coal-Fired Power Plant. *Industrial & Engineering Chemistry Research* **58**, 15533-15541, doi:10.1021/acs.iecr.9b02253 (2019).

8 Zijlema, T. G., Geertman, R. M., Witkamp, G.-J., van Rosmalen, G. M. & de Graauw, J. Antisolvent Crystallization as an Alternative to Evaporative Crystallization for the Production of Sodium Chloride. *Industrial & Engineering Chemistry Research* **39**, 1330-1337, doi:10.1021/ie990221h (2000).

9 LLC, I. S. *Sodium Bicarbonate Prices*, <https://www.intratec.us/solutions/primary-commodity-prices/commodity/sodium-bicarbonate-prices> (2026).

10 LLC, I. S. *Soda Ash (Sodium Carbonate) Prices*, <https://www.intratec.us/solutions/primary-commodity-prices/commodity/soda-ash-prices> (2026).

11 Rabinowitz, J. A. & Kanan, M. W. The future of low-temperature carbon dioxide electrolysis depends on solving one basic problem. *Nature Communications* **11**, doi:10.1038/s41467-020-19135-8 (2020).

12 Ma, M. *et al.* Insights into the carbon balance for CO_2 electroreduction on Cu using gas diffusion electrode reactor designs. *Energy & Environmental Science* **13**, 977-985, doi:10.1039/d0ee00047g (2020).

13 Shin, H., Hansen, K. U. & Jiao, F. Techno-economic assessment of low-temperature carbon dioxide electrolysis. *Nature Sustainability* **4**, 911-919, doi:10.1038/s41893-021-00739-x (2021).

14 Bertuccioli, L. *et al.* Development of water electrolysis in the European Union. (2014).

15 Richardson, I. A. *et al.* Low-cost, transportable hydrogen fueling station for early market adoption of fuel cell electric vehicles. *International Journal of Hydrogen Energy* **40**, 8122-8127, doi:10.1016/j.ijhydene.2015.04.066 (2015).